

STRONG DEPENDENCE OF THE INNER EDGE OF THE HABITABLE ZONE ON PLANETARY ROTATION RATE

JUN YANG¹, GWENAËL BOUÉ^{2,3}, DANIEL C. FABRYCKY², AND DORIAN S. ABBOT¹

¹ Department of Geophysical Sciences, University of Chicago, Chicago, IL 60637, USA; abbot@uchicago.edu

² Department of Astronomy and Astrophysics, University of Chicago, Chicago, IL 60637, USA

³ Sorbonne Universités, IMCCE, Observatoire de Paris, UPMC Univ. Paris 06, UMR 8028, F-75014 Paris, France

Received 2014 March 31; accepted 2014 April 16; published 2014 April 25

ABSTRACT

Planetary rotation rate is a key parameter in determining atmospheric circulation and hence the spatial pattern of clouds. Since clouds can exert a dominant control on planetary radiation balance, rotation rate could be critical for determining the mean planetary climate. Here we investigate this idea using a three-dimensional general circulation model with a sophisticated cloud scheme. We find that slowly rotating planets (like Venus) can maintain an Earth-like climate at nearly twice the stellar flux as rapidly rotating planets (like Earth). This suggests that many exoplanets previously believed to be too hot may actually be habitable, depending on their rotation rate. The explanation for this behavior is that slowly rotating planets have a weak Coriolis force and long daytime illumination, which promotes strong convergence and convection in the substellar region. This produces a large area of optically thick clouds, which greatly increases the planetary albedo. In contrast, on rapidly rotating planets a much narrower belt of clouds form in the deep tropics, leading to a relatively low albedo. A particularly striking example of the importance of rotation rate suggested by our simulations is that a planet with modern Earth's atmosphere, in Venus' orbit, and with modern Venus' (slow) rotation rate would be habitable. This would imply that if Venus went through a runaway greenhouse, it had a higher rotation rate at that time.

Key words: astrobiology – planets and satellites: atmospheres – planets and satellites: detection

Online-only material: color figures

1. INTRODUCTION

It is traditional to define the habitable zone based on whether liquid water can be maintained on a planet's surface, which is primarily controlled by the planet's surface temperature (TS; Kasting et al. 1993, 2014). Accurate estimates of the stellar flux boundaries of the habitable zone are critical for estimating parameters of astrophysical interest such as the frequency of Earth-like planets (e.g., Kopparapu 2013). The inner edge of the habitable zone is set by the runaway greenhouse effect, a positive feedback through which an entire ocean can be evaporated into the atmosphere (Nakajima et al. 1992). Our ability to constrain the stellar flux corresponding to the inner edge of the habitable zone has been severely hampered by the inability of one-dimensional (1D) radiative–convective models to predict cloud behavior (Selsis et al. 2007).

Clouds are critical to planetary energy balance. Cloud reflection of solar radiation is responsible for most of the planetary albedo on modern Earth (Donohoe & Battisti 2011), and clouds also significantly increase Earth's greenhouse effect by absorbing terrestrial infrared emission (Harrison et al. 1990). Cloud coverage and location are primarily controlled by large-scale atmospheric circulation, which is determined by a variety of factors including stellar flux, orbital parameters, and rotation rate. As the stellar flux increases, cloud coverage and thickness may increase, potentially leading to a higher albedo and a negative feedback, or decrease, potentially leading to a lower albedo and a positive feedback.⁴ Orbital parameters such as obliquity and eccentricity can both drive large-amplitude sea-

sonal cycles of the atmospheric circulation and TS (e.g., Ferreira et al. 2014), but they tend to minimally affect the annual-mean climate (Williams & Pollard 2002, 2003).

Planetary rotation rate determines the strength of the Coriolis force (the apparent force felt due to the rotation of the planet) and the length of day (and night). The Coriolis force is a key parameter in determining the atmospheric circulation (e.g., Schneider 2006; Showman et al. 2013). If the Coriolis force is strong, thermally direct latitudinal circulations (Hadley cells) are constrained to low latitudes, and the atmosphere organizes into banded, roughly longitudinally symmetric regions. If the Coriolis force is weak, horizontal temperature gradients become small throughout the atmosphere and the Hadley cells can extend globally. The length of day, combined with surface and atmospheric thermal inertia, helps determine the TS distribution, which drives atmospheric circulation (Pierrehumbert 2010). For a short day (or large thermal inertia), the TS difference between day and night is small. If the day is long enough that the dayside is much warmer than the nightside, atmospheric circulation is characterized by ascent on the warm dayside and descent on the cold nightside.

Recently a number of calculations have been done with three-dimensional (3D) general circulation models (GCMs) to assess the effects of atmospheric circulation, subsaturation, and clouds on the inner edge of the habitable zone (Yang et al. 2013; Leconte et al. 2013a; Wolf & Toon 2014). In the extreme case of tidally locked synchronously rotating planets orbiting M stars, strong atmospheric ascent on the dayside leads to thick dayside cloud coverage and a very high planetary albedo (Yang et al. 2013). This can allow a planet to remain habitable at twice the stellar flux 1D model calculations would suggest. In contrast, for rapidly rotating planets with banded atmospheric circulations, cloud behavior remains roughly similar to modern

⁴ Here we assume that changes in cloud reflection of stellar radiation (cooling) dominate over changes in cloud absorption of planetary infrared radiation (warming), which is the case in the simulations we present below.

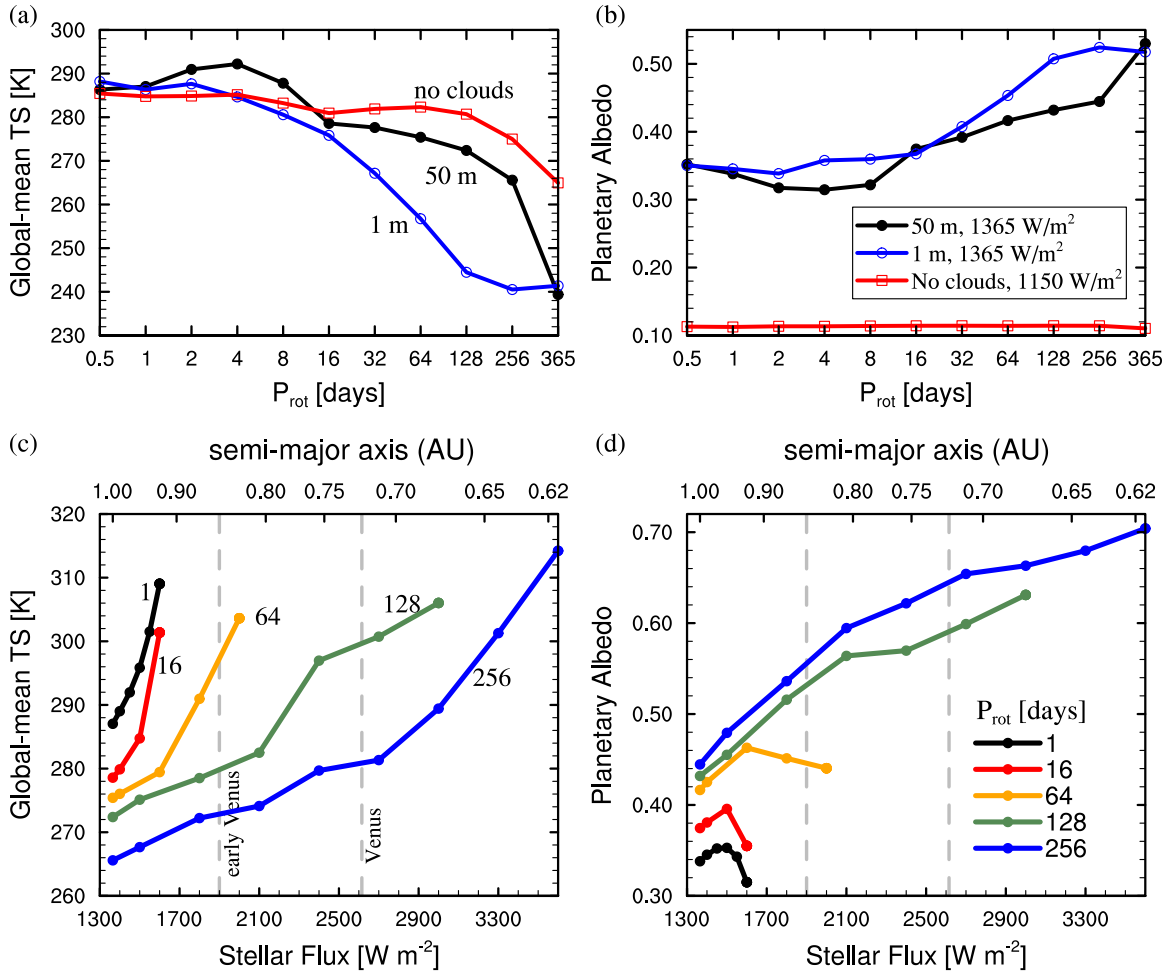


Figure 1. Dependence of planetary climate on rotation period (P_{rot}) for planets orbiting a Sun-like star. ((a) and (b)) Global-mean TS and planetary albedo as a function of P_{rot} for a given stellar flux (S_0). Black line: $S_0 = 1365 \text{ W m}^{-2}$ and the surface heat capacity (D) is equivalent to 50 m of water; blue line: $S_0 = 1365 \text{ W m}^{-2}$ and $D = 1 \text{ m}$; red line: clouds are switched off, $S_0 = 1150 \text{ W m}^{-2}$, and $D = 50 \text{ m}$. For $P_{\text{rot}} = 365$ days, the planet is in a synchronously rotating state. ((c) and (d)) Global-mean TS and planetary albedo as a function of stellar flux (S_0) for a given P_{rot} with $D = 50 \text{ m}$. The vertical dashed lines denote the stellar flux of early and modern Venus. The upper horizontal axis in panels (c) and (d) is the corresponding semi-major axis between a Sun-like star and the planet in AU. In all these simulations the orbital period is 365 days and there is no sea ice.

(A color version of this figure is available in the online journal.)

Earth’s (which the albedo of 1D models are tuned to) so that the inner edge of the habitable zone in 3D models is similar to that in 1D models (Leconte et al. 2013a; Wolf & Toon 2014). Another interesting difference is that the cloud feedback near the runaway greenhouse threshold appears to be negative for tidally locked planets (Yang et al. 2013) and positive for rapidly rotating planets (Leconte et al. 2013a; Wolf & Toon 2014).⁵

The purpose of this study is to investigate the effects of a range of planetary rotation rates, between tidally locked and rapidly rotating, and stellar types on cloud behavior and the inner edge of the habitable zone. To do this we use a 3D GCM with a sophisticated cloud scheme that reproduces cloud behavior well in the large range of climates observed on modern Earth. Although we do not push the model significantly outside of this range, it is important to note that cloud modeling is difficult, and other models may yield quantitatively different results. Nevertheless, we focus on results due to robust physical processes that should be qualitatively similar in any 3D model. Our main conclusion is that for all stellar types slowly rotating

planets (orbital period ≈ 100 days or more) behave similarly to tidally locked planets and have a high planetary albedo near the inner edge of the habitable zone. The width of the habitable zone is therefore strongly dependent on planetary rotation rate.

2. METHODS

For most of the results presented below we use the Community Atmosphere Model version 3.1 (CAM3; Collins et al. 2004), which is a 3D atmospheric GCM that was developed by the National Center for Atmospheric Research to simulate the climate of Earth. CAM3 calculates atmospheric circulation and radiative transfer, and uses subgrid-scale parameterizations to model small-scale vertical convection, clouds, and precipitation. We perform additional simulations in some cases using the Community Atmosphere Model version 4.0 (CAM4; Neale et al. 2010) and the Community Climate System Model version 3.0 (CCSM3; Collins et al. 2006). CCSM3 is a coupled ocean–atmosphere model that calculates ocean circulation explicitly and uses CAM3 as its atmospheric component. We run CAM3 and CAM4 coupled to an immobile ocean with a uniform depth and a uniform albedo of 0.06. The GCMs simulate

⁵ Wolf & Toon (2014) find a cloud feedback that starts negative, then becomes positive near the runaway greenhouse.

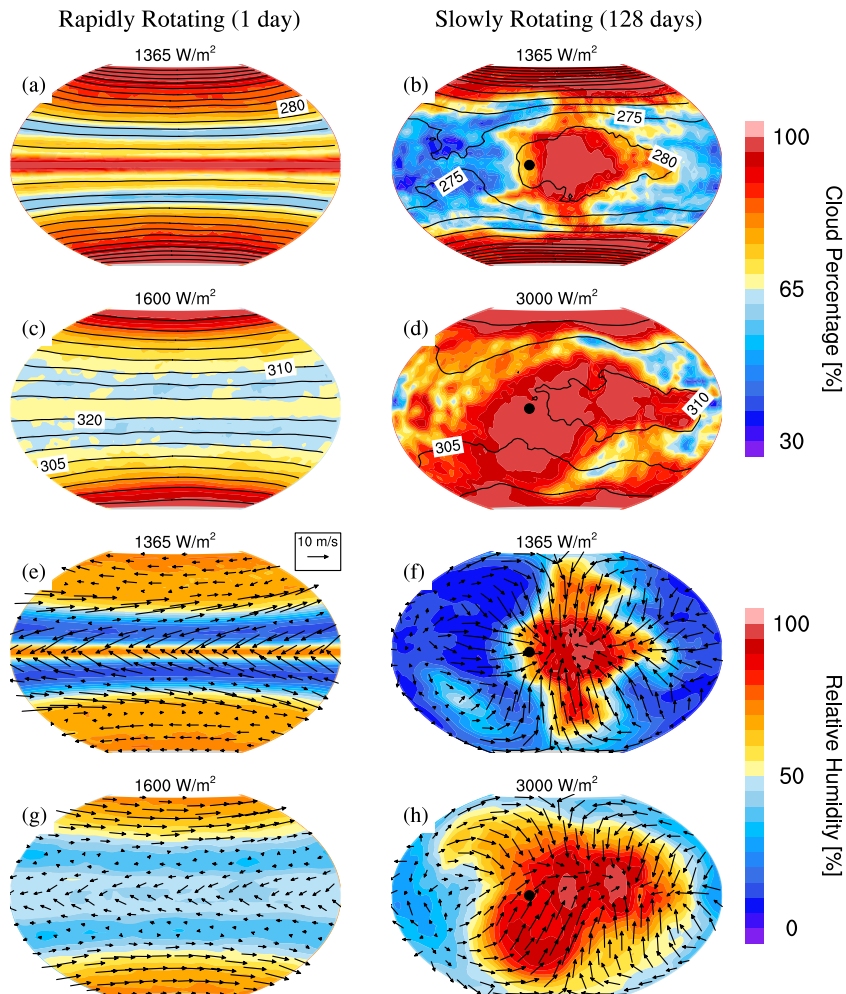


Figure 2. Differences in clouds and atmospheric circulation between rapidly (left) and slowly (right) rotating planets with an orbital period of 365 days. The rotation period is 1 day for the rapidly rotating planet and the stellar flux is 1365 or 1600 W m^{-2} . The rotation period is 128 days for the slowly rotating planet and the stellar flux is 1365 or 3000 W m^{-2} . ((a)–(d)) Total cloud coverage (%; shaded) and TS (K; black contours with an interval of 5 K). ((e)–(h)) Relative humidity at 450 mbar (%; shaded) and near-surface winds (m s^{-1} , vectors). The black dot in the right panels is the transient substellar point, which moves westward around the planet with a period of 197 days. All variables are averaged over 30 days.

(A color version of this figure is available in the online journal.)

marine stratus, layered, shallow convective, and deep convective clouds as well as prognostically calculate liquid and ice cloud condensate. Compared to CAM3, CAM4 has a revised deep convection scheme and a similar cloud scheme. The default atmospheric pressure we use is 1.0 bar (mainly N_2), with $\text{CO}_2 = 400$ ppmv and $\text{CH}_4 = 1$ ppmv. We set geothermal heat flux, aerosols, obliquity, and eccentricity to zero. We run CAM3 at a horizontal resolution of $3^\circ 75' \times 3^\circ 75'$ with 26 vertical levels from the surface to ≈ 30 km.

In our simulations where we change the rotation rate and increase the stellar flux we use Earth’s planetary parameters, including radius (R_\oplus), gravity (g_\oplus), and orbital period (P_{orb} , 365 days). We increase the stellar flux until the model crashes, which occurs when the global-mean TS reaches ≈ 310 K. Comparison with the clear-sky calculations of Leconte et al. (2013a) shows agreement between CAM3 and generic-Laboratoire de Météorologie Dynamique (LMD) to within ≈ 5 K up to this temperature. We use the last converged solution as a proxy for the inner edge of the habitable zone. We examine a series of rotation periods (P_{rot}) ranging from 12 hr to 365 days. We perform simulations using the Sun’s spectrum and stellar spectra corresponding to M (blackbody 3400 K), K (4500 K), and F (6800 K)

stars. In our simulations examining a planet with Venus’ orbital characteristics and Earth’s atmosphere, we use a stellar flux $S_0 = 2615 \text{ W m}^{-2}$, $P_{\text{orb}} = 225$ days, $P_{\text{rot}} = -243$ days (retrograde rotation), $R_p = 0.95 R_\oplus$, and $g_p = 0.9 g_\oplus$. Our default simulation in this case uses Earth’s continental configuration with continents composed of clay and sand (albedo = 0.2, thermal conductivity = $0.26 \text{ W m}^{-1} \text{ K}^{-1}$).

3. DRAMATIC EFFECT OF PLANETARY ROTATION

For a given stellar flux (S_0), the TS of rapidly rotating planets is much higher than that of slowly rotating planets (Figure 1(a)). When we use a surface heat capacity equivalent to 50 m of water ($D = 50$ m), the global-mean TS decreases by 20 K when we increase the rotation period (P_{rot}) from 1 day to 256 days, and then decreases by another 25 K when the planet becomes tidally locked ($P_{\text{rot}} = 365$ days). The primary reason for this is that the cloud albedo is much higher on slowly rotating planets (Figure 1(b)). If we artificially set clouds to zero in the model, TS is nearly independent of rotation rate, except for the tidally locked and nearly tidally locked cases (Figure 1(a)). TS is lower in these cases because a thermal inversion on the nightside leads

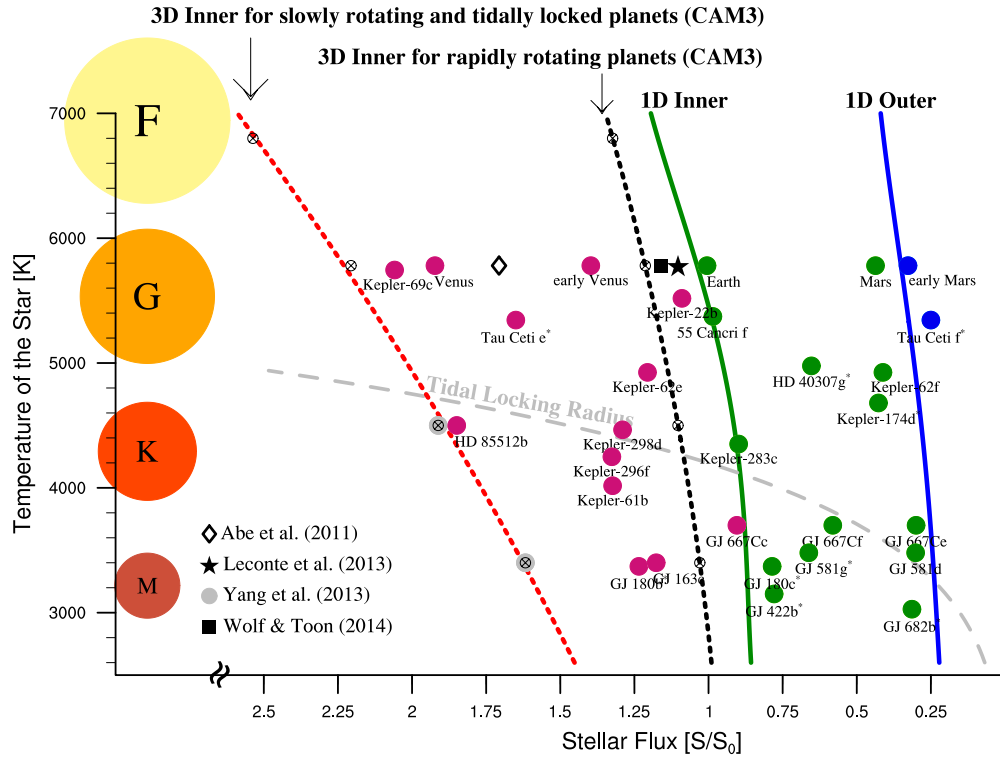


Figure 3. Habitable zone boundaries as a function of stellar type and planetary rotation rate for a 1D radiative-convective model and for the 3D general circulation model CAM3. Blue line: the 1D outer edge (maximum greenhouse; Kopparapu et al. 2013); green line: the 1D inner edge (runaway greenhouse; Kopparapu et al. 2013); black line: the 3D inner edge for rapidly rotating planets in CAM3 (rotation period of 1 day); red line: the 3D inner edge for slowly rotating planets in CAM3 (rotation period of 128 days for G and F stars, and tidally locked with an orbit of 60 days for M and K stars); gray line: the tidal locking radius (Kasting et al. 1993). The CAM3 simulations used to calculate the 3D inner edge lines are denoted by \otimes . We also plot the inner edge of the habitable zone for rapidly rotating dry planets (Abe et al. 2011), for Earth obtained in generic-LMD (Leconte et al. 2013a) and CAM3 with a modified radiative-transfer module (Wolf & Toon 2014). Finally, we plot solar system planets and discovered exoplanets (unconfirmed exoplanets are marked by *).

(A color version of this figure is available in the online journal.)

to a radiator fin that cools the planet (Yang et al. 2013; Yang & Abbot 2014). If we reduce D to 1 m, the TS distribution is able to adjust to the moving stellar forcing so that the planet can behave as if it were tidally locked even when P_{rot} is decreased to 128 days (Figure 1). When $D = 50$ m, TS has a maximum at $P_{\text{rot}} = 4$ days that appears to be associated with a high latitude cloud feedback similar to that described by Abbot & Tziperman (2008).

There is a dramatic difference between the response of the planetary albedo to increases in S_0 for rapidly and slowly rotating planets. For rapidly rotating planets, as S_0 increases the planetary albedo first increases, then decreases (Figure 1(d)), leading to a positive feedback near the runaway greenhouse threshold (Leconte et al. 2013a; Wolf & Toon 2014). This positive feedback is due to a combination of decreased cloud reflection and increased water vapor absorption. In contrast, for slowly rotating planets, the planetary albedo monotonously increases with S_0 , leading to a negative feedback that stabilizes the climate. For rapidly rotating planets, the atmospheric circulation is banded and Earth-like. This leads to high cloud coverage both in a tropical convergence zone associated with the ascent of the Hadley cells (Figure 2(e)) and at higher latitudes associated with baroclinic eddies (Figure 2(a)). The tropical clouds are most important for planetary albedo because the stellar flux is highest there. As S_0 increases, the equator-to-polar temperature gradient decreases (Figure 2(c)), which weakens the Hadley cells (Held & Hou 1980), reduces tropical cloud coverage (Figure 2(c)), and decreases the planetary albedo (Figure 1(d)). For slowly rotating planets, a global atmospheric circulation occurs with

strong low-level convergence and ascent in the (slowly moving) substellar region (Figure 2(f)) similar to the circulation on synchronously rotating planets (Joshi et al. 1997; Showman et al. 2013; Leconte et al. 2013b). This circulation leads to strong convection and optically thick clouds (Figure 2(b)) in the substellar region (Yang et al. 2013). As S_0 increases the circulation weakens, but the zone of ascent spreads out, which leads to a broader area of high relative humidity (Figure 2(h)) and high cloud coverage (Figure 2(d)). Additionally, the cloud water content increases, making individual clouds optically thicker. As a result, the planetary albedo increases with S_0 (Figure 1(d)).

Our simulations indicate that the inner edge of the habitable zone is strongly dependent on planetary rotation rate. Numerous discovered exoplanets that were previously considered uninhabitable may be within the habitable zone⁶ if they rotate slowly (Figure 3). Our simulations yield an inner edge of the habitable zone for rapidly rotating planets approximated by the curve

$$S_{\text{rap}} = 1.2138 + 9.8344 \times 10^{-5} (T_{\text{eff}} - 5780) + 8.8000 \times 10^{-9} (T_{\text{eff}} - 5780)^2,$$

and for slowly rotating planets

$$S_{\text{slow}} = 2.2296 + 2.8056 \times 10^{-4} (T_{\text{eff}} - 5780) + 1.1308 \times 10^{-8} (T_{\text{eff}} - 5780)^2,$$

⁶ Our simulations generally have low stratospheric water vapor (Table 1), but a full investigation of water loss on slowly rotating planets is beyond the scope of this Letter.

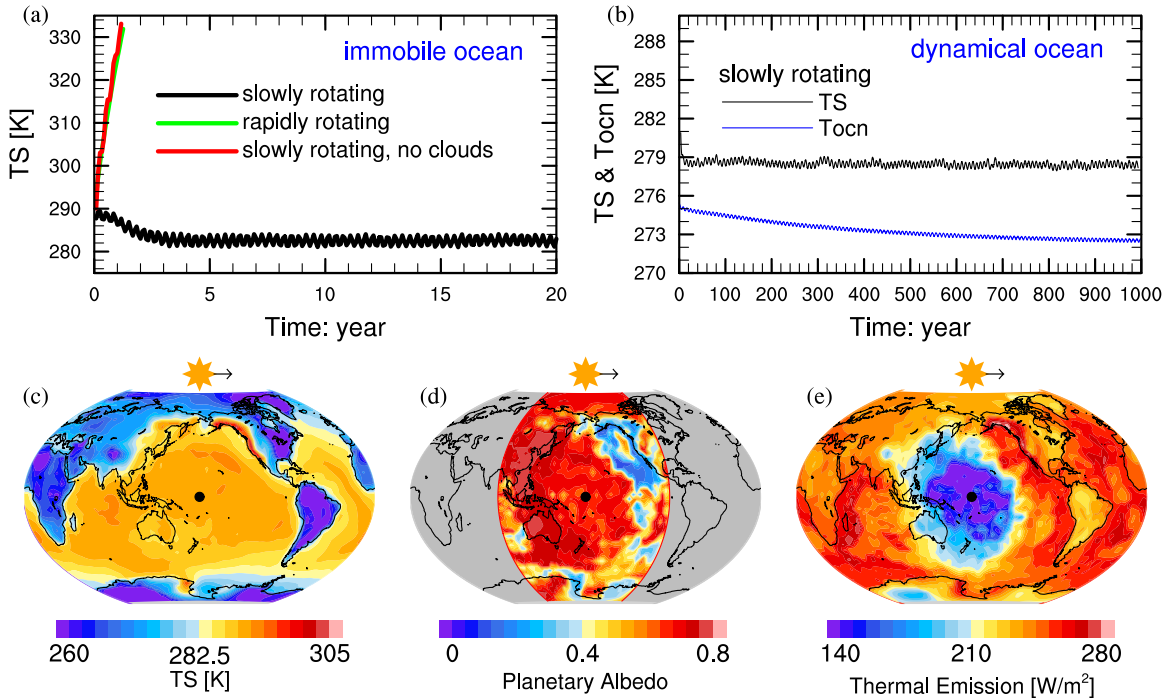


Figure 4. Climate of a planet with modern Earth’s atmosphere and continental configuration, but in Venus’ orbit and with Venus’ (slow) rotation rate. (a) Time series of global-mean TS simulated by the atmospheric model CAM3 for Venus’ rotation rate (slowly rotating, black), Earth’s rotation rate (rapidly rotating, green), and Venus’ rotation rate with clouds artificially set to zero (slowly rotating, no clouds, red). The planet quickly tends toward a runaway greenhouse if it is rapidly rotating or has no clouds, but is habitable if it is slowly rotating. (b) Global-mean TS and vertically integrated ocean temperature (Toccn) in a coupled ocean–atmosphere simulation using CCSM3 and Venus’ rotation rate. ((c)–(e)) Maps of TS, planetary albedo, and thermal emission to space averaged over 1 day in the coupled CCSM3 simulation. The black dot in panels (c)–(e) is the transient substellar point, which moves eastward around the planet with a period of 117 days.

(A color version of this figure is available in the online journal.)

where S_{rap} and S_{slow} are stellar fluxes divided by 1360 W m^{-2} and T_{eff} is the temperature of the star. We note that our S_{rap} is slightly larger than that of Wolf & Toon (2014), who also use CAM3, but have implemented a more sophisticated radiative transfer scheme, and use different surface boundary conditions, orbital parameters, and trace gas concentrations (Figure 3). Although the values of S_{rap} and S_{slow} estimated using different GCMs and assumptions will likely differ by $\approx 10\%$, the robust cloud processes we describe should always make S_{slow} significantly larger than S_{rap} .

Our results suggest that a planet at Venus’ distance from a Sun-like star could be habitable if it rotated slowly and had an Earth-like atmosphere.⁷ We checked this using CCSM3 to simulate the climate a planet like Earth would have with Venus’ present orbital parameters and rotation rate ($P_{\text{rot}} = -243$ days). Although the stellar flux is 1.92 times modern Earth’s, the planetary albedo is 0.65 so that the planet absorbs slightly less radiation than modern Earth and the maximum TS is only 306 K (Figure 4). The slow rotation and consequent stabilizing cloud feedback are the keys to preventing the planet from entering a runaway greenhouse at this high stellar flux. If either P_{rot} is decreased to 1 day or the clouds are switched off, the model tends toward a runaway greenhouse (Figure 4(a)). Further simulations show that the planet tends toward a runaway greenhouse if either the day length or the Coriolis parameter are changed to be Earth-like (and the other is held constant). We have performed a large variety of sensitivity tests that demonstrate the robustness of our conclusion that an Earth-like planet in Venus’ orbit would

likely be habitable (Table 1). These ideas could eventually be tested by using the *James Webb Space Telescope* to look for weak thermal emission at the substellar point (Figure 4(e)) of detected exoplanets (Yang et al. 2013).

Our work has important implications for the evolution of Venus. Deuterium enrichment in Venus’ atmosphere suggests that it may have started with an ocean and gone through a runaway greenhouse (Donahue et al. 1982). Our results suggest that if the runaway happened near the beginning of the solar system, Venus would have had to have a rotation period less than a few weeks, and if the runaway occurred recently, Venus would have had to have a rotation period less than a few months (Figure 1, Table 1). Any water would then be photodissociated and lost to space, and large amounts of CO_2 would accumulate in the atmosphere since silicate weathering would not occur if there were no surface water (Kasting 2010). Tidal interactions could later slow Venus’ rotation rate to its present value (Correia & Laskar 2001), but it would be too late for Venus to return to habitable conditions. If instead all of the water on Venus were lost through hydrodynamic escape during formation and Venus did not start with oceans (Hamano et al. 2013), then the rotation rate would not need to have changed over its history.

Consideration of Venus shows that slowly rotating planets which our calculations suggest *could* be habitable will not actually be habitable in *all* cases. This will depend on whether they started with a rapid rotation rate, and if so, how long it took for their rotation rate to slow, the rate of water loss if they entered a runaway greenhouse at some point in their history, their (possible) migration history, and the timing and amount of volatile delivery, among other things. This is no different from any previous estimate of habitable zone, since it has always

⁷ We note that Leconte et al. (2013a) speculate that rotation rate could be important for the history of habitability on Venus.

Table 1
Simulated Climates of a Planet with Venus' Orbit and (Slow) Rotation Rate and with an Earth-like Atmosphere

Group	Model	Experimental Design	α_p^a (0–1)	G^b (K)	$V(\text{H}_2\text{O})^c$ (ppmv)	TS ^d (K)
1 ^e	CAM3	Default (Earth's continental configuration)	0.64	30	1.8	282
1	CAM3	No continents (aqua-planet)	0.58	39	6.5	303
1	CAM4	No continents (aqua-planet)	0.59	38	49	300
1	CCSM3	Dynamical ocean	0.64	24	152	278
1	CCSM3	Dynamical ocean (4 km), no continents	0.64	29	0.4	283
2 ^f	CAM3	Default (Earth's continental configuration)	0.65	31	2.0	284
2	CAM3	Switch off sea ice module	0.65	31	2.0	284
2	CAM3	No continents (aqua-planet)	0.59	41	7.5	303
2	CAM3	No continents, increase the model resolution	0.62	46	137	307
2	CAM3	Decrease the model time step	0.64	32	2.1	284
2	CAM3	Cloud ice particle size $\times 0.5$	0.66	32	10	282
2	CAM3	Cloud ice particle size $\times 2.0$	0.63	31	0.6	285
2	CAM3	Cloud liquid particle size $\times 0.5$	0.67	29	0.5	276
2	CAM3	Cloud liquid particle size $\times 2.0$	0.58	43	454	306
2	CAM3	Decrease the mixed layer depth to 1 m	0.64	26	4.1	280
2	CAM3	Increase the mixed layer depth to 200 m	0.65	31	1.6	283
2	CAM3	Increase the mixed layer depth to 500 m	0.65	32	1.7	284
2	CAM3	Increase the CO ₂ concentration to 0.1 bars	0.63	56	158	310
2	CAM3	Increase the surface pressure to 2 bars	0.65	36	0.3	287
2	CAM3	Increase the surface pressure to 5 bars	0.65	49	0.3	301
2	CAM3	Increase gravity to 1.5 g_{\oplus}	0.64	29	0.7	283
2	CAM3	Increase the radius to 2.0 R_{\oplus}	0.65	31	2.0	284
2	CAM3	Increase the obliquity from 0° to 23°5	0.65	31	1.9	283
2	CAM3	Increase the eccentricity from 0 to 0.2	0.61	41	611	301
3 ^g	CAM3	$S_0 = 1900 \text{ W m}^{-2}$, $P_{\text{rot}} = 8$ days		Tends to runaway warming		
3	CAM3	$S_0 = 1900 \text{ W m}^{-2}$, $P_{\text{rot}} = 16$ days	0.46	41	0.6	301
3	CAM3	$S_0 = 2615 \text{ W m}^{-2}$, $P_{\text{rot}} = 32$ days		Tends to runaway warming		
3	CAM3	$S_0 = 2615 \text{ W m}^{-2}$, $P_{\text{rot}} = 48$ days	0.63	32	2.4	287

Notes. By default, $S_0 = 2615 \text{ W m}^{-2}$, $P_{\text{rot}} = -243$ days, and $P_{\text{orb}} = 225$ days.

^a α_p : planetary albedo.

^b G : global-mean greenhouse effect.

^c $V(\text{H}_2\text{O})$: stratospheric vapor content in units of parts per million by volume (ppmv).

^d TS: global-mean surface temperature.

^e Group 1: $p\text{CO}_2 = 400$ ppmv, $p\text{CH}_4 = 1$ ppmv, $p\text{N}_2\text{O} = 0$.

^f Group 2: $p\text{CO}_2 = 500$ ppmv, $p\text{CH}_4 = 10$ ppmv, $p\text{N}_2\text{O} = 1$ ppmv.

^g Group 3: same as default sets of Group 1, except varying S_0 and/or P_{rot} .

been understood that habitability depends on planetary history in addition to location.

4. CONCLUSION

This work demonstrates that the inner edge of the habitable zone for slowly rotating planets could be at twice the stellar flux as for rapidly rotating planets. Numerical simulations suggest that the rotation periods of planets at formation could vary between 10 hr and 400 days (Miguel & Brunini 2010), and tidal interactions can further slow planetary rotation (Lago & Cazenave 1979). It is therefore probable that a large number of planets rotate slowly enough to have a greatly expanded habitable zone. Additionally, our simulations suggesting that an Earth-like planet with Venus' present orbit and rotation rate would be habitable demonstrate that empirical limits on the habitable zone based on solar system planets (e.g., Kasting et al. 2014) may not be as strong constraints as previously believed, depending on factors such as rotation rate and planetary history. Finally, we note that although we expect our results to be qualitatively robust, the details will differ with other models that have different cloud and radiation schemes. We can hope to resolve this issue by comparing GCMs, applying cloud resolving

models to the problem (e.g., Abbot 2014), and eventually observing planets using methods such as those suggested by Yang et al. (2013).

We are grateful to D. Koll, Y. Wang, Y. Liu, F. Ding, C. Zhou, and C. Bitz for technical assistance and/or helpful discussions. D.S.A. acknowledges support from an Alfred P. Sloan Research Fellowship. This work was completed in part with resources provided by the University of Chicago Research Computing Center.

REFERENCES

- Abbot, D. S. 2014, *JCLI*, in press
 Abbot, D. S., & Tziperman, E. 2008, *QJRM*, **134**, 165
 Abe, Y., Abe-Ouchi, A., Sleep, N. H., & Zahnle, K. J. 2011, *Asbio*, **11**, 443
 Collins, W. D., Basch, P. J., Boville, B. A., et al. 2004, Technical Note, Document NCAR-TN-464+STR (Boulder, CO: NCAR),
 Collins, W. D., Bitz, C. M., Blackmon, M. L., et al. 2006, *JCLI*, **19**, 2122
 Correia, A. C. M., & Laskar, J. 2001, *Natur*, **411**, 767
 Donahue, T. M., Hoffman, J. H., Hodges, R. R., & Watson, A. J. 1982, *Sci*, **216**, 630
 Donohoe, A., & Battisti, D. S. 2011, *JCLI*, **24**, 4402
 Ferreira, D., Marshall, J., O'Gorman, P. A., & Seager, S. 2014, Ica, submitted
 Hamano, K., Abe, Y., & Genda, H. 2013, *Natur*, **497**, 607
 Harrison, E. F., Minnis, P., Barkstrom, B. R., et al. 1990, *JGR*, **95**, 18687

- Held, I. M., & Hou, A. Y. 1980, *JAtS*, **37**, 515
- Joshi, M. M., Haberle, R. M., & Reynolds, R. T. 1997, *Icar*, **129**, 450
- Kasting, J. F. 2010, *How to Find a Habitable Planet* (Princeton, NJ: Princeton Univ. Press)
- Kasting, J. F., Kopparapu, R., Ramirez, R. M., & Harman, C. E. 2014, *PNAS*, in press
- Kasting, J. F., Whitmire, D. P., & Reynolds, R. T. 1993, *Icar*, **101**, 108
- Kopparapu, R. K. 2013, *ApJL*, **767**, L8
- Kopparapu, R. K., Ramirez, R., Kasting, J. F., et al. 2013, *ApJ*, **767**, 131
- Lago, B., & Cazenave, A. 1979, *M&P*, **21**, 127
- Leconte, J., Forget, F., Charnay, B., Wordsworth, R., & Pottier, A. 2013a, *Natur*, **504**, 268
- Leconte, J., Forget, F., Charnay, B., et al. 2013b, *A&A*, **554**, A69
- Miguel, Y., & Brunini, A. 2010, *MNRAS*, **406**, 1935
- Nakajima, S., Hayashi, Y.-Y., & Abe, Y. 1992, *JAtS*, **49**, 2256
- Neale, R. B., Richter, J. H., Conley, A. J., et al. 2010, Technical Note, Document NCAR-TN-485+STR (Boulder, CO: NCAR)
- Pierrehumbert, R. T. 2010, *Principles of Planetary Climate* (Cambridge: Cambridge Univ. Press)
- Schneider, T. 2006, *AREPS*, **34**, 655
- Selsis, F., Kasting, J. F., Levrard, B., et al. 2007, *A&A*, **476**, 1373
- Showman, A. P., Wordsworth, R. D., Merlis, T. M., & Kaspi, Y. 2013, in *Comparative Climatology of Terrestrial Planets*, ed. S. J. Mackwell, A. A. Simon-Miller, J. W. Harder, & M. A. Bullock (Tucson, AZ: Univ. Arizona Press), 277
- Williams, D. M., & Pollard, D. 2002, *IAsb*, **1**, 61
- Williams, D. M., & Pollard, D. 2003, *IAsb*, **2**, 1
- Wolf, E. T., & Toon, O. B. 2014, *GeoRL*, **41**, 167
- Yang, J., & Abbot, D. S. 2014, *ApJ*, **784**, 155
- Yang, J., Cowan, N. B., & Abbot, D. S. 2013, *ApJL*, **771**, L45